Molecular orbital view of the electronic coupling between two metal nanoparticles

M. Claudia Troparevsky,[1,2] Ke Zhao,[1,2,3] Di Xiao,[2] Adolfo G. Eguiluz,[1,2] and Zhenyu Zhang[2,1,4]
[1]*Department of Physics and Astronomy, The University of Tennessee, Knoxville, Tennessee 37996, USA*
[2]*Materials Science and Technology Division, Oak Ridge National Laboratory, Oak Ridge, Tennessee 37831, USA*
[3]*Department of Mechanical Engineering and Materials Science, Rice University, Houston, Texas 77005, USA*
[4]*ICQD, University of Science and Technology of China, Hefei, Anhui, 230026, China*
(Received 17 April 2010; revised manuscript received 15 June 2010; published 15 July 2010)

The electronic coupling between metal nanoparticles is responsible for intriguing new phenomena observed when the particles are near touching contact, which is exemplified by recent investigations of nanoparticle dimers. However, little is known about the role of the molecular orbitals of the nanoparticle dimers. The expectation is that the physics and chemistry of the system must be reflected in the orbitals that control the bonding at touching contact. This expectation is borne out in the present investigation in which we present a comprehensive theoretical study based on density-functional theory of the electronic coupling between two silver nanoparticles. We explain our findings by studying the molecular orbitals of the dimers as a function of the separation and relative orientation between the nanoparticles. We show that as the nanoparticles approach each other a bond-forming step takes place, and that the strength of the hybridization is a key element to determine various properties of the system. We find that the relative orientation between the nanoparticles plays an important role in determining the strength of the coupling which can be visualized by the spatial distribution of the highest occupied molecular orbitals. Moreover, the strength of the coupling will in turn determine the ease of their transition to the nonlinear dielectric-response regime. This effect allows for the tunability of the electronic coupling and magnetic moment of the dimer. Our findings are essential for understanding and tailoring desired physical and chemical properties of closely aggregated nanoparticles relevant for applications such as surface-enhanced Raman scattering and quantum transport in molecular devices.

DOI: 10.1103/PhysRevB.82.045413 PACS number(s): 36.40.Cg, 75.75.−c

I. INTRODUCTION

Nanoparticles have recently become the focus of intense interest due to their unique physical and chemical properties, which can be very different from those of atoms or bulk phase.[1–6] Most importantly, the possibility of tuning selected properties of the nanoparticles has led to intriguing insights into the physics of materials at the nanoscale.[7–9] The vast interest in nanoparticles goes beyond the properties of isolated particles; indeed this interest extends to their potential to form self-organized films and solids.[10,11] Nanoparticle aggregates have also gained increased attention since interesting phenomena have been reported as the nanoparticles are allowed to come close to each other. For example, an insulator-to-metal transition has been observed in nanoparticle superlattices as the distance between the nanoparticles is decreased;[12] also by varying the interparticle separation of a nanoparticle dimer to dimensions much smaller than that of the particles, strongly enhanced optical responses have been achieved.[13–15] In addition, compact three-dimensional superlattices of magnetic nanoparticles have drawn great interest for applications in high-density magnetic recording.[16,17] As new applications demand the nanoparticles to be more densely packed, the understanding of the impact of the electronic coupling on the chemical and physical properties of nanoparticle arrays is a key to tailor the desired properties of these systems.

The study of the electronic coupling between nanoparticles near touching contact and the analysis of the evolution of their molecular orbitals as the separation between the particles is decreased is still in need of further investigation. There have been some theoretical studies that focus on the electronic coupling between two metal nanoparticles. Most of the existing studies have used either classical or simplified jellium models.[18–21] Recently, the importance of quantum-mechanical effects in the optical response of nanoparticles near touching contact has been pointed out.[22,23] Even for nanoparticles with radii in the tens of nanometers, the optical response is significantly affected when the separation between the nanoparticles is below 1 nm. In addition, *ab initio* studies on silver nanoparticle dimers showed the relevance of the coupling between the metal nanoparticle and the molecule in the gap region on the surface-enhanced Raman scattering (SERS) enhancements.[24,25] This important effect could only be captured by a realistic quantum-mechanical study of the system.

The role of *ab initio* studies to accurately describe the coupling between metal nanoparticles was also verified by our recent study of silver nanoparticle dimers.[26] We showed the relevant role of the electronic coupling between two metal nanoparticles in determining the response of the system to an applied electric field. We found that the electronic coupling depends on both the separation and the relative orientation between the particles. We showed that as the two particles are separated from touching contact, the dimer undergoes a bond-breaking step, which also establishes the existence of an optimal gap size (OGS) defined by a maximal static polarizability of the dimer. For some dimers, the electronic coupling before the bond breaks can be strong enough to give rise to a net magnetic moment of the dimer, even though the isolated particles are nonmagnetic. Furthermore, we have recently showed that the electronic coupling and magnetic moment of a metal nanoparticle dimer can be

readily tuned by applying an electric field once the system is in the nonlinear dielectric-response regime.[27] This shows the critical role of the wave-function overlap between the nanoparticles and how the bonding between the particles can drastically change the response of the dimers to an applied electric field.

There have been several experimental studies where the coupling of nanoparticles and the formation of bonding and antibonding orbitals has been evidenced. In particular, it has been observed that as the coupling between the nanoparticles is increased, the sharp resonance from the exciton transition of an isolated particle splits into a pair of lines.[28] This splitting is a clear evidence of the formation of a bonding and antibonding states. More recently, the delocalized molecular states of coupled InAs nanoparticles have been studied. It has been shown that the nature of the molecular ground state changes from bonding to antibonding as the coupling between the nanoparticles is decreased.[29]

The main question that arises is if molecules composed of nanoparticles are just a rescaled version of their atomic counterparts or if these "artificial molecules" offer novel properties. Therefore, a realistic understanding of the interparticle coupling and the study of the molecular orbitals when the nanoparticles are in close proximity is of critical significance in both fundamental studies and applications of nanotechnology.

In this paper, we present a detailed study of the electronic coupling between two silver nanoparticles using *ab initio* density-functional theory (DFT). We study the evolution of the molecular orbitals of the dimers as a function of the separation between the nanoparticles and the interplay between the electronic coupling and the response of the system to an applied electric field. We investigate the coupling between the nanoparticles as a function of the separation between the nanoparticles, (dimer gap size), and relative orientation of the nanoparticles. We show that as the nanoparticles approach each other they form a bond which is evidenced by the emergence of a delocalized highest occupied molecular orbital (HOMO). We also investigate the transition of the dimer systems to the nonlinear dielectric-response regime from a molecular orbital view. By looking at the HOMOs and the lowest unoccupied molecular orbitals (LUMOs) of the dimers as a function of the electric field, a field-induced level crossing can be demonstrated once the dimer is in the nonlinear response regime. The field-induced level crossing, which is evidenced by the change in character of the HOMO and the LUMO—from symmetric to antisymmetric—as the magnitude of the field is increased, results in the emergence of a net magnetic moment of the dimer.

The paper is organized as follows. In Sec. II, we present the computational methods. The study of the dimer wave functions and the bonding between the metal nanoparticles as a function of the gap size and different relative orientations in the absence of an external electric field are presented in Sec. III. The effect of applying an external electric field on the bonding between the nanoparticles and the transition of the dimers to the nonlinear dielectric-response regime is discussed in Sec. IV. Our discussion is presented in Sec. V and conclusions are summarized in Sec. VI.

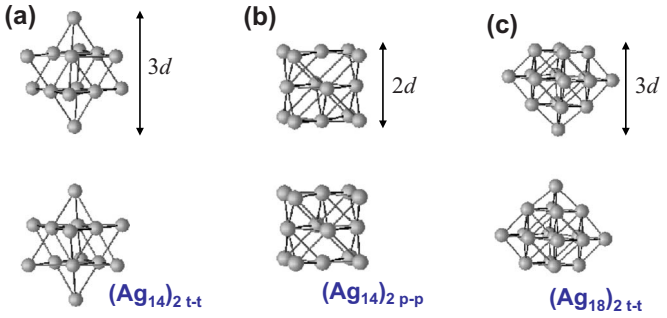

FIG. 1. (Color online) Atomic configurations of the silver nanoparticle dimers. (a) $(Ag_{14})_2$ with t-t orientation, (b) $(Ag_{14})_2$ with p-p orientation, and (c) $(Ag_{18})_2$ with t-t orientation. The dimer axis is along [111] in the t-t and [100] in the p-p orientation of $(Ag_{14})_2$, and [100] in both the t-t and p-p orientations of $(Ag_{18})_2$.

II. COMPUTATIONAL METHODS

Our DFT calculations were performed within the local spin-density approximation (LSDA), using the Ceperley-Alder exchange-correlation functional,[30] parametrized by Perdew and Zunger.[31] The Kohn-Sham equations are discretized and solved on a three-dimensional uniform grid, using the higher-order finite-difference method in real space.[32,33] We used improved Troullier-Martins pseudopotentials[34] in the nonlocal form, generated from the $4d^{10}5s^{1}5p^{0}$ configuration of Ag with core radii $r_{cs}=r_{cp}=r_{cd}=2.34$ a.u. We used a 0.32 a.u. grid spacing for the structural minimizations and a grid spacing of 0.4 a.u. for the calculations of the polarizabilities. The clusters were placed in a spherical domain whose radius was chosen so that no atom is within 11.5 a.u. of the domain boundary. The wave functions were required to vanish outside this domain.

For the calculations of the static polarizability, the external field is introduced in the Hamiltonian by adding a term to the Kohn-Sham potential,

$$\left[-\frac{\hbar^2\nabla^2}{2m}+V_{eff}(\boldsymbol{r})-e\boldsymbol{F}\cdot\boldsymbol{r}\right]\phi_i(\boldsymbol{r})=\varepsilon_i\phi_i(\boldsymbol{r}), \tag{1}$$

where $\phi_i(\boldsymbol{r})$ and ε_i are the single-particle eigenfunctions and eigenvalues, and $V_{eff}(\mathbf{r})$ includes the ionic, Hartree, and exchange-correlation terms. By the self-consistent solution of Eq. (1), we determine both the dipole moment and the total energy as a function of the applied electric field. The diagonal elements of the polarizability tensor α_{ij} can be found using the finite-difference expressions for the first and second derivatives, according to

$$\alpha_{ij}=\frac{\partial\mu_i(\boldsymbol{F})}{\partial F_i}=\frac{\partial^2E(\boldsymbol{F})}{\partial F_i\,\partial F_j},\quad i,j=\{x,y,z\}, \tag{2}$$

where $\mathbf{F}$ is the applied uniform electric field.

The polarizability can be calculated either from the dipole moment or from the total energy at $F=0$, and $F=\pm\delta F_i$ applied along the ith axis. In this work, we present the values of the polarizability calculated from the dipole moment. We only apply the electric field along the z axis, which is the axis

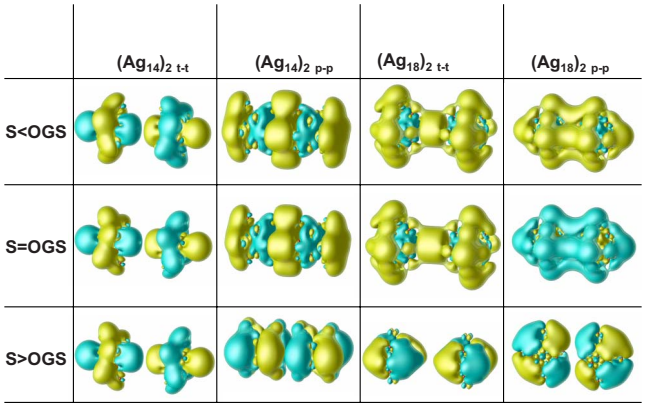

FIG. 2. (Color online) Highest occupied wave function of $(Ag_{14})_{2\ t\text{-}t}$, $(Ag_{14})_{2\ p\text{-}p}$, $(Ag_{18})_{2\ t\text{-}t}$, and $(Ag_{18})_{2\ p\text{-}p}$ for gap sizes smaller, equal, and larger than the OGS. The yellow color indicates positive values and the green color indicates negative values of the wave functions. All the wave functions in our calculations are real.

along which the clusters face each other. The results reported for the static polarizability are then only the α_{zz} element of the polarizability tensor.

Here we study systems consisting of two 18-atom and two 14-atom silver nanoparticles with two different orientations, tip-tip (t-t), and plane-plane (p-p), (see Fig. 1). The nanoparticles are a fragment of the Ag bulk in the fcc structure. The coordinates of each individual cluster have been relaxed so that the maximum magnitude of the force on any atom is smaller than 0.07 eV/Å. The dimers will be referred to as $(Ag_n)_2$, where n is the number of atoms in each nanoparticle. We note that the average layer thickness d of the nanoparticles is d=2.2 Å for $(Ag_{14})_{2\ t\text{-}t}$, 2.0 Å for $(Ag_{14})_{2\ p\text{-}p}$, and 1.9 Å for $(Ag_{18})_2$ along both orientations.

III. BONDING BETWEEN TWO METAL NANOPARTICLES

We have recently shown[26] that the electronic coupling between metal nanoparticle dimers is manifested by their linear response to an applied electric field. As two silver nanoparticles approach each other the static polarizability of the dimer increases until it reaches a maximum at an OGS.[26] The underlying physical picture behind these findings is as follows: at small separations, bellow the OGS, the nanoparticles are strongly coupled and there is significant overlap of the wave functions of the neighboring atoms. The wave-function overlap between the nanoparticles constitutes a channel through which charge can flow freely, and the polarizability increases as the gap size increases. Beyond the OGS, the overlap vanishes and the charge flow is discontinued. In this regime, the contribution of the electromagnetic coupling becomes dominant and consequently the polarizability decreases as the gap size increases. In the following, we offer a molecular orbital view of the above physical picture.

Figure 2 shows the highest occupied wave function of $(Ag_{14})_{2\ t\text{-}t}$, $(Ag_{14})_{2\ p\text{-}p}$, $(Ag_{18})_{2\ t\text{-}t}$, and $(Ag_{18})_{2\ p\text{-}p}$ at the OGS, and for separations below and beyond the OGS (all our wave functions happen to be real). For $(Ag_{14})_{2\ p\text{-}p}$, $(Ag_{18})_{2\ t\text{-}t}$, and $(Ag_{18})_{2\ p\text{-}p}$ a significant wave-function overlap is observed at the OGS which translates into a bonding HOMO which is delocalized over the two nanoparticles. In all three cases, a strong wave-function overlap is present which gives rise to a hybridization of the orbitals of the individual clusters to form a bond at the OGS. On the other hand, $(Ag_{14})_{2\ t\text{-}t}$ presents a small wave-function overlap at the OGS and it does not present a hybridization of the orbitals to form a strong bond between the nanoparticles. The bond-forming step is also evident by looking at the symmetry properties of the HOMO. The HOMO of $(Ag_{14})_{2\ t\text{-}t}$ is antisymmetric and its character remains unchanged as a function of the gap size S. On the other hand, $(Ag_{14})_{2\ p\text{-}p}$, $(Ag_{18})_{2\ t\text{-}t}$, and $(Ag_{18})_{2\ p\text{-}p}$ present a symmetric HOMO which becomes antisymmetric beyond the OGS indicating a bond-breaking step.

The effect of the bond-forming step can be observed from Fig. 3. This figure shows the polarizability of $(Ag_{18})_{2\ t\text{-}t}$ vs S, which clearly displays a maximum at S=3.17 Å (OGS). The bond-breaking/bond-forming step can be seen from the insets in Fig. 3. For separations smaller and up to the OGS, the

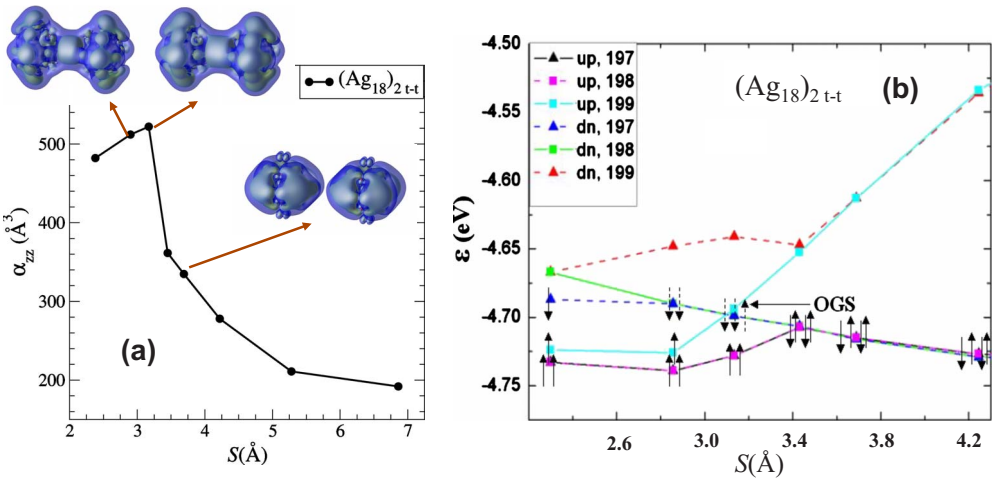

FIG. 3. (Color online) (a) Static polarizability of $(Ag_{18})_{2\ t\text{-}t}$ for several gap sizes, S. Insets: $|\mathrm{HOMO}|^2$ of $(Ag_{18})_{2\ t\text{-}t}$ for S=2.64 Å, S=3.17 Å, which corresponds to the OGS, and S=3.71 Å. (b) Energy levels around HOMO-LUMO gap of $(Ag_{18})_{2\ t\text{-}t}$ for several gap sizes S. A solid arrow pointing up (down) means a spin-up (down) level has an occupation of one while a dotted arrow indicates a fractionally occupied level. The numbers following "up" and "down" correspond to occupied or unoccupied energy levels.

dimer presents a bond between the nanoparticles which is evidenced by the spatial distribution of its HOMO. For separations slightly larger than the OGS, (~0.5 Å beyond the OGS), the character of the HOMO changes dramatically and it now resembles that of the two isolated nanoparticles. $(Ag_{14})_{2\ p\text{-}p}$ and $(Ag_{18})_{2\ p\text{-}p}$ present a similar behavior of the polarizability vs S while the curve for $(Ag_{14})_{2\ t\text{-}t}$ has a less pronounced peak.

A consequence of the hybridization between the orbitals of the nanoparticles is the closing of the HOMO-LUMO gap of the dimer system at the OGS [see Fig. 3(b)]. The closing of the HOMO-LUMO gap and eventually the crossing of the HOMO and the LUMO can be observed from Fig. 2. Since the system always has mirror symmetry with respect to the middle plane between the two particles, the parity of the HOMO cannot change unless the energy levels cross at some point. It can be deduced from Fig. 2 that the level crossing occurs for $(Ag_{14})_{2\ p\text{-}p}$, $(Ag_{18})_{2\ t\text{-}t}$, and $(Ag_{18})_{2\ p\text{-}p}$ since the parity of the HOMO changes at the OGS.

The relative orientation between the nanoparticles also plays a key role in determining the strength of the coupling, which cannot be explained solely by the number of atoms that face each other as the nanoparticles approach. The strength of the bonding between the nanoparticles can be clearly seen from Fig. 2 where the HOMO at the OGS is plotted for each dimer. For instance, the most striking difference is found for the Ag_{14} dimers. The p-p orientation presents a bond at the OGS while the t-t orientation only presents a weak overlap of the wave functions in the gap region. This difference is also reflected in the response of the system to an applied electric field.

It is noteworthy to note that the polarizabilities of a single Ag_{14} along the [111] and [100] directions are almost identical, (they differ by less than 1%), regardless of the anisotropic shape of the nanoparticle. However, the orientation dependence becomes very significant when the two Ag_{14} clusters are in close proximity. For the same particle size, the t-t orientation has a higher value of the maximum polarizability and a smaller OGS. This behavior can be explained by looking at the HOMOs of both the isolated nanoparticle and the dimer in both orientations. The HOMO for the isolated Ag_{14} has a spherical shape which explains why the polarizability has almost identical values in both [111] and [100] directions. On the other hand, the shape of the HOMO of the dimer at small gap sizes differs in shape significantly between the t-t and the p-p orientations.

$(Ag_{14})_{2\ t\text{-}t}$ presents a special case among the dimers studied here since it is the only one which does not present a significant hybridization of the orbitals or a formation of a bond. Unlike the other cases, the HOMO of $(Ag_{14})_{2\ t\text{-}t}$ resembles two orbitals from independent clusters facing each other. A consequence of the lack of hybridization between the orbitals of the Ag_{14} clusters in the t-t orientation, and therefore the small overlap of the orbitals at the center of the gap region, is that the HOMO-LUMO gap of $(Ag_{14})_{2\ t\text{-}t}$ remains finite as the particles approach each other. This is in sharp contrast to the other dimers studied here, where the formation of a bonding and antibonding orbitals closes the HOMO-LUMO gap at the OGS. The absence of the closing of the HOMO-LUMO gap for $(Ag_{14})_{2\ t\text{-}t}$ explains why it is the only dimer that does not present an emergence of a net magnetic moment below the OGS.

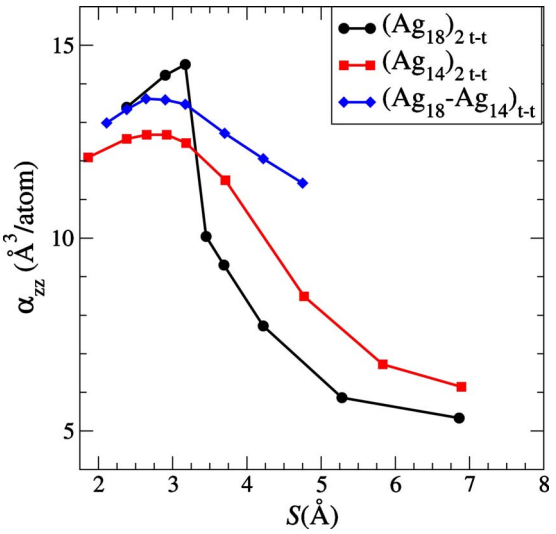

FIG. 4. (Color online) Static polarizability per atom of $(Ag_{18})_{2\ t\text{-}t}$, $(Ag_{14})_{2\ t\text{-}t}$, and $(Ag_{18}\text{-}Ag_{14})_{t\text{-}t}$ as a function of S.

Given the inertness of the Ag_{14} cluster in the t-t orientation, we studied a dimer system composed of one Ag_{18} and one Ag_{14} facing each other in the t-t orientation $(Ag_{18}\text{-}Ag_{14})_{t\text{-}t}$. Figure 4 shows the polarizability vs S for $(Ag_{18})_{2\ t\text{-}t}$, $(Ag_{14})_{2\ t\text{-}t}$, and $(Ag_{18}\text{-}Ag_{14})_{t\text{-}t}$. It can be seen from this figure that for the case of $(Ag_{14})_{2\ t\text{-}t}$, the decrease in the polarizability with increasing S is much smoother than in the case of $(Ag_{18})_{2\ t\text{-}t}$. $(Ag_{18}\text{-}Ag_{14})_{t\text{-}t}$ represents an intermediate case, and it is important to note that although the HOMO-LUMO gap for this system decreases as the particles approach, there is no emergence of a net magnetic moment below the OGS. Indeed, the dimer presents a small but finite HOMO-LUMO gap (0.1 eV) at the OGS. This can serve as additional evidence of the inertness of the t-t orientation for Ag_{14}. The orbitals of this heterodimer resemble either the ones of an isolated Ag_{14} or the ones of an isolated Ag_{18}, and there is no evidence of a strong hybridization that would allow the formation of a bond as in the case of $(Ag_{18})_{2\ t\text{-}t}$. The HOMO for this heterodimer is mostly localized on the Ag_{18} cluster with some minor delocalization over the gap region.

IV. INTERPLAY BETWEEN THE ELECTRIC FIELD AND THE BONDING BETWEEN TWO NANOPARTICLES

A. Transition to the nonlinear dielectric-response regime

We have recently shown that the nanoparticle dimers transition to the nonlinear dielectric-response regime for modest values of the electric field. Once the dimer system is in the nonlinear dielectric-response regime its electronic coupling and magnetic moment can be tuned by applying an electric field.[27] Hence, we start by studying the effect of applying an electric field on the molecular orbitals of the dimer and on the bonding between the nanoparticles. We first calculate P/E and the spatial distribution of the wave functions for

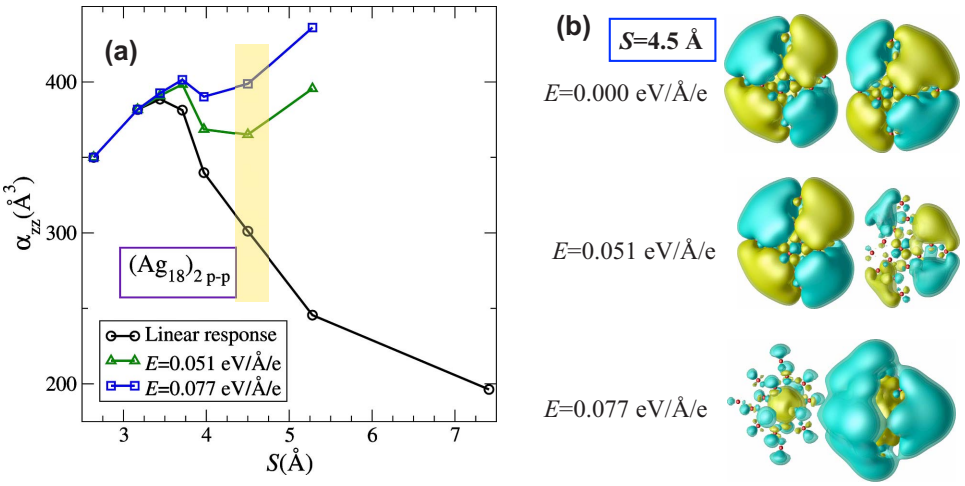

FIG. 5. (Color online) (a) P/E of $(Ag_{18})_{2\ p\text{-}p}$ as a function of S for the linear-response regime, and for $E=0.051$, and 0.077 eV/Å/e. (b) Real part of the HOMO of $(Ag_{18})_{2\ p\text{-}p}$ at $S=4.50$ Å for $E=0.026$ (linear-response regime), 0.051, and 0.077 eV/Å/e.

several gap sizes, S, and several values of the electric field E, where P is the dipole moment of the dimer.

Figure 5(a) shows the P/E curves vs S of $(Ag_{18})_{2\ p\text{-}p}$ for several values of the electric field. From these curves, it can be observed that P/E for different values of E coincide with each other and with the curve dP/dE obtained from a linear-response calculation when the separation is smaller than the OGS. The system deviates from the linear-response curve immediately upon further increase in the separation ($S>$OGS).

Remarkably, the transition to the nonlinear regime occurs for modest values of the electric field for all dimers studied here. As a reference, the isolated Ag_{18} cluster remains in the linear-response regime with applied electric fields of magnitudes of up to 0.5 eV/Å/e. For the cases of $(Ag_{18})_{2\ t\text{-}t}$ and $(Ag_{18})_{2\ p\text{-}p}$, the system transitions to the nonlinear response regime for very small magnitudes of the field once the dimer is beyond the OGS. In particular, for $(Ag_{18})_{2\ t\text{-}t}$, beyond the OGS the dimer is in the nonlinear response regime even for the smallest field we can apply in our numerical studies. We would like to note that although LSDA is well known to underestimate the HOMO-LUMO gap, the phenomena reported herein would still occur if the correct values of the gaps were used but at slightly larger field strengths.

The transition to the nonlinear response regime can also be explained from the change in the character of the HOMO of the dimer as the magnitude of the electric field is increased. Figure 5(b) shows the highest occupied wave function of $(Ag_{18})_{2\ p\text{-}p}$ at $S=4.50$ Å for $E=0$, 0.051, and 0.077 eV/Å/e. It can be seen from Fig. 5(a) that $S=4.50$ Å is larger than the OGS, and that the system is in the nonlinear response regime for $E=0.051$ and 0.077 eV/Å/e. For $E=0$, the wave function is antisymmetric and for $E=0.051$ eV/Å/e, the character of the HOMO has not changed although it has been distorted by the applied electric field. On the other hand, for $E=0.077$ eV/Å/e, the character of the HOMO has changed and, as in the case of $E=0.051$ eV/Å/e, it is considerably distorted by the electric field. This change in character of the highest occupied wave function is a clear indication not only of the transition to the nonlinear response regime but of a level crossing induced by the applied electric field.

B. Magnetic moment

Here, we demonstrate, by studying the evolution of the wave functions and the energy levels of the dimer as a function of the applied electric field, that indeed the electric field causes the HOMO-LUMO gap to decrease. Moreover, it eventually causes the HOMO and LUMO to cross each other, leading to a net magnetic moment of the dimer.

Figure 6(a) shows the HOMO and LUMO of $(Ag_{14})_{2\ p\text{-}p}$ at $S=3.70$ Å for $E=0$ and $E=0.31$ eV/Å. The level-crossing effect can be observed from the change in character of the HOMO and LUMO as the magnitude of the electric field is increased. For $E=0$ the HOMO of $(Ag_{14})_{2\ p\text{-}p}$ is antisymmetric and mostly localized on the individual nanoparticles. The LUMO of the dimer is symmetric, delocalized over the two nanoparticles, and presents significant overlap in the gap region. On the other hand, for $E=0.31$ eV/Å, the HOMO is delocalized over the two nanoparticles while the LUMO is mostly localized over the individual nanoparticles, clearly displaying the field-induced level crossing.

A consequence of the field-induced level crossing is the change in the magnetic moment of the dimer as the magnitude of the electric field is increased. Figure 6(b) shows the net magnetic moment of $(Ag_{18})_{2\ p\text{-}p}$ and $(Ag_{14})_{2\ p\text{-}p}$ as a function of the applied electric field for a fixed S. The gap sizes, $S=3.97$ Å for $(Ag_{18})_{2\ p\text{-}p}$ and $S=3.70$ Å for $(Ag_{14})_{2\ p\text{-}p}$, are both larger than their respective OGS. Indeed the magnetic moment for both dimers can be tuned from $0\mu_B$ to $2\mu_B$ as the electric field is increased from $E=0$ to $E=0.31$ eV/Å/e. For the three cases, $(Ag_{18})_{2\ p\text{-}p}$, $(Ag_{14})_{2\ p\text{-}p}$, and $(Ag_{18})_{2\ t\text{-}t}$, in which the dimers present a strong hybridization of the orbitals below the OGS, the net magnetic moment can be tuned by modest magnitudes of the electric field for S beyond the OGS. For instance, for the case of $(Ag_{18})_{2\ p\text{-}p}$ at the OGS the magnetic moment remains constant at $2\mu_B$ for all the magnitudes of the electric field plotted in Fig. 6.

The shift of the energy levels for $(Ag_{14})_{2\ p\text{-}p}$ at $S=4.50$ Å, as the electric field is increased from zero to 0.31 eV/Å/e can be seen from Fig. 6(c). At $E=0$, the dimer presents a finite HOMO-LUMO gap, equal occupation numbers for spin-up and spin-down levels, and therefore a zero net magnetic moment. As the magnitude of the electric field

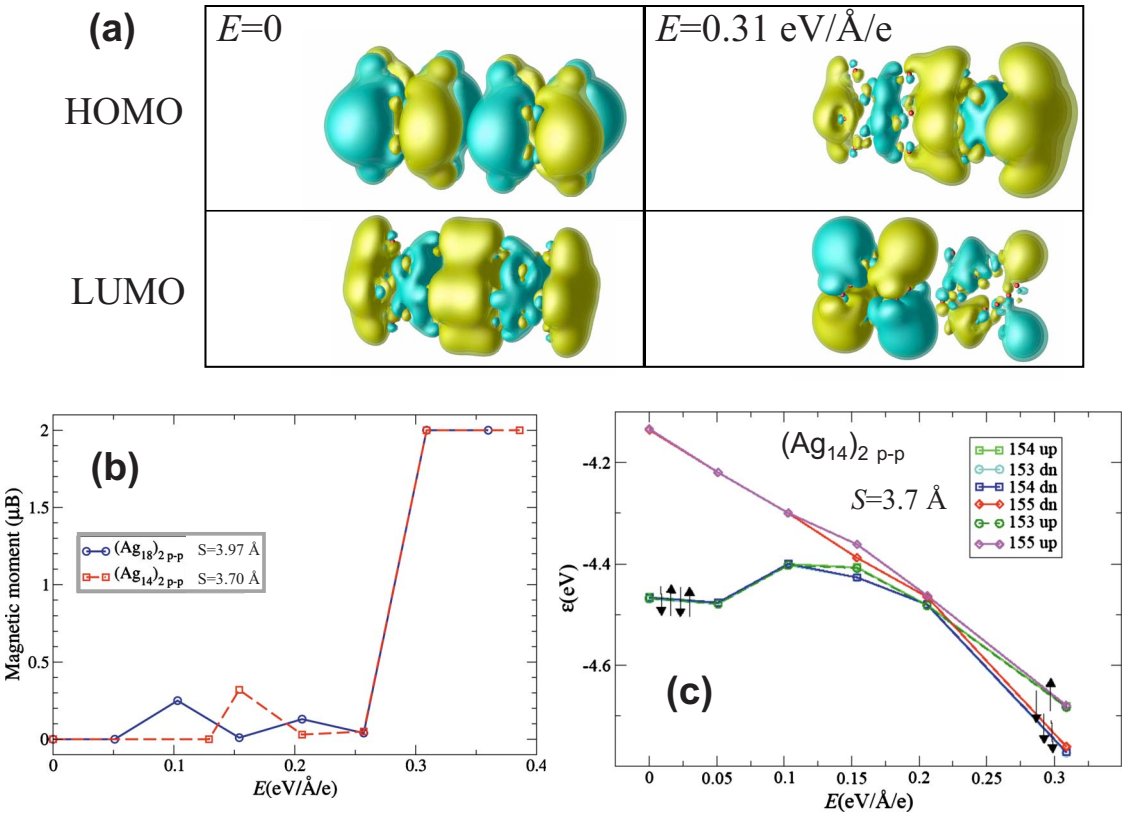

FIG. 6. (Color online) (a) HOMO and LUMO of $(Ag_{14})_{2\ p\text{-}p}$ for $S=3.70$ Å at $E=0$ and at $E=0.31$ eV/Å/e. (b) Net magnetic moment of $(Ag_{14})_{2\ p\text{-}p}$ and $(Ag_{18})_{2\ p\text{-}p}$ as a function of the applied electric field for $S=3.70$ Å and $S=3.97$ Å, respectively. (c) Energy levels around the HOMO-LUMO gap of $(Ag_{14})_{2\ p\text{-}p}$ as a function of the applied electric field for $S=3.70$ Å. An arrow pointing up (down) means a spin-up (down) level is occupied. The numbers following up and down correspond to occupied or unoccupied energy levels.

increases, the HOMO-LUMO gap decreases and the degeneracy between spin-up and spin-down levels is lifted. Eventually, the HOMO-LUMO gap closes, and further increase in the electric field causes the HOMO and LUMO to cross each other leading to a net magnetic moment of $2\mu_B$.

V. DISCUSSION

The effect of the electronic coupling between the nanoparticles on their magnetic properties and its potential tunability is a key for new technological applications. Examples of these applications are the compact three-dimensional superlattices of magnetic nanoparticles and their use in data-storage devices.[11] Also, the emergence of a net magnetic moment due to the level-crossing effect, points out a possible way to generate spin-polarized current and stresses the delicate interplay between the electronic and magnetic degrees of freedom in these nanostructures. The tunability of the magnetic moment through an applied electric field also gives rise to the possibility of making tunable multifunctional devices. Currently, two types of systems are being investigated for the search of new multiferroic materials: bulk materials[35] and thin-film heterostructures.[36] Our findings indicate that nanoparticle aggregates can emerge as a potential new class of multiferroic materials. In addition, nanoparticles present several advantages over the conventional bulk materials due to the extra degrees of freedom they possess, such as the size of the nanoparticles, their relative orientation, and the gap size.

For SERS applications, the bond-forming step between the nanoparticles is the relevant feature since it affects the static polarizability of the dimer. A similar effect would be expected for the dynamic polarizability of the system which will determine its optical response. The inclusion of a molecule in the gap region between the nanoparticles is expected to further modify the electronic coupling and it is the focus of a forthcoming work.

The formation of a bond between the nanoparticles, and consequently the formation of a bonding and antibonding orbitals can have important consequences on the charge-transfer process within nanoparticle arrays since it may cause the decrease in the HOMO-LUMO gap. The relevance of the HOMO-LUMO gap and the electronic coupling have been pointed out in the electron transport within atomic chain systems and single conjugated organic molecules,[37,38] and in the charge transfer between semiconducting nanoparticles.[39,40] Our results show that the relative orientation between the nanoparticles is essential to determine the strength of the coupling, and in addition it can be tuned by varying the magnitude of the applied electric field. Moreover, our findings are very relevant for the investigation of quantum transport in molecular devices.[41–45] When a molecule is trapped between two metal nanostructures or leads, the assumption that the system is in the linear-response regime should be

taken with great caution since, as we have shown, a small bias voltage may lead to nonlinear behavior.

In addition, the change in character of the HOMO of the dimer caused by the electronic coupling between the nanoparticles can have important consequences in the chemical reactivity of these systems. The adsorption of a molecule on a metal nanoparticle could be altered by modifying the coupling between the nanoparticles. The tunability of the coupling between the nanoparticles can be achieved by varying the gap size or, for a fixed gap size, by applying an electric field. The tunability of the chemical reactivity of strongly coupled nanoparticles is the focus of ongoing work.

VI. CONCLUSIONS

In summary, we have performed first-principles calculations based on density-functional theory to study the electronic coupling between silver nanoparticles of different sizes and with different relative orientations. By studying the molecular orbitals of the dimers as a function of the separation between the nanoparticles, we found that as the nanoparticles approach each other they form a bond. The formation of the bond is responsible for the formation of a bonding and antibonding orbitals which may close the HOMO-LUMO gap of the dimer and consequently give rise to a net magnetic moment of the system below its OGS. We also showed that the strength of the hybridization is very dependent on the relative orientation between the nanoparticles. The formation of a delocalized HOMO at the OGS is also manifested in the response of the system to an applied electric field, displayed by the presence of a maximum in the static polarizability as a function of the separation between nanoparticles. The coupling between the nanoparticles causes the system to transition to the nonlinear dielectric-response regime for modest values of the electric field. Once the dimer is in the nonlinear-response regime further increase in the electric field may make the HOMO and LUMO cross each other giving rise to a net magnetic moment of the dimer. The field-induced level crossing is demonstrated by the change in character of the HOMO of the dimer as the magnitude of the field is increased.

ACKNOWLEDGMENTS

This work was supported in part by NSF (Grant Nos. DMR-0906025 and OCI-0904972), and by DOE (the Division of Material Sciences and Engineering, Office of Basic Sciences, and BES-CMSN). K.Z. at Rice University was supported by the Robert Welch Foundation (C-1590). The calculations were performed at NERSC.

[1] A. P. Alivisatos, Science **271**, 933 (1996).
[2] R. J. Warburton, C. Schäflein, D. Haft, F. Bickel, A. Lorke, K. Karrai, J. M. Garcia, W. Schoenfeld, and P. M. Petroff, Nature (London) **405**, 926 (2000).
[3] S. R. Nicewarner-Peña, R. G. Freeman, B. D. Reiss, L. He, D. J. Peña, I. D. Walton, R. Cromer, C. D. Keating, and M. J. Natan, Science **294**, 137 (2001).
[4] C. J. Murphy and J. L. Coffer, Appl. Spectrosc. **56**, 16A (2002).
[5] K. L. Kelly, E. Coronado, L. L. Zhao, and G. C. Schatz, J. Phys. Chem. B **107**, 668 (2003).
[6] S. Eustis and M. A. El-Sayed, Chem. Soc. Rev. **35**, 209 (2006).
[7] K. A. Willets and R. P. Van Duyne, Annu. Rev. Phys. Chem. **58**, 267 (2007).
[8] J. N. Anker, W. P. Hall, O. Lyandres, N. C. Shah, J. Zhao, and R. P. Van Duyne, Nat. Mater. **7**, 442 (2008).
[9] H. Nakanishi, K. J. M. Bishop, B. Kowalczyk, A. Nitzan, E. A. Weiss, K. V. Tretiakov, M. M. Apodaca, R. Klajn, J. F. Stoddart, and B. A. Grzybowski, Nature (London) **460**, 371 (2009).
[10] S. Sun, C. B. Murray, D. Weller, L. Folks, and A. Moser, Science **287**, 1989 (2000).
[11] C. Desvaux, C. Amiens, P. Fejes, P. Renaud, M. Respaud, P. Lecante, E. Snoeck, and B. Chaudret, Nature Mater. **4**, 750 (2005).
[12] C. P. Collier, R. J. Saykally, J. J. Shiang, S. E. Henrichs, and J. R. Heath, Science **277**, 1978 (1997).
[13] H. X. Xu, E. J. Bjerneld, M. Käll, and L. Börjesson, Phys. Rev. Lett. **83**, 4357 (1999).
[14] A. M. Michaels, J. Jiang, and L. Brus, J. Phys. Chem. B **104**, 11965 (2000).
[15] E. Prodan, C. Radloff, N. J. Halas, and P. Nordlander, Science **302**, 419 (2003).
[16] D. E. Speliotis, J. Magn. Magn. Mater. **193**, 29 (1999).
[17] S. A. Majetich and Y. Jin, Science **284**, 470 (1999).
[18] H. X. Xu, J. Aizpurua, M. Käll, and P. Apell, Phys. Rev. E **62**, 4318 (2000).
[19] J. Jiang, K. Bosnick, M. Maillard, and L. Brus, J. Phys. Chem. B **107**, 9964 (2003).
[20] I. Grigorenko, S. Haas, and A. F. J. Levi, Phys. Rev. Lett. **97**, 036806 (2006).
[21] I. Grigorenko, S. Haas, A. Balatsky, and A. F. J. Levi, New J. Phys. **10**, 043017 (2008).
[22] F. J. García de Abajo, J. Phys. Chem. C **112**, 17983 (2008).
[23] J. Zuloaga, E. Prodan, and P. Nordlander, Nano Lett. **9**, 887 (2009).
[24] L. L. Zhao, L. Jensen, and G. C. Schatz, Nano Lett. **6**, 1229 (2006).
[25] L. Jensen, C. M. Aikens, and G. C. Schatz, Chem. Soc. Rev. **37**, 1061 (2008).
[26] K. Zhao, M. C. Troparevsky, D. Xiao, A. G. Eguiluz, and Z. Zhang, Phys. Rev. Lett. **102**, 186804 (2009).
[27] M. C. Troparevsky, K. Zhao, D. Xiao, Z. Zhang, and A. G. Eguiluz, Nano Lett. **9**, 4452 (2009).
[28] G. Schedelbeck, W. Wegscheider, M. Bichler, and G. Abstreiter, Science **278**, 1792 (1997).
[29] M. F. Doty, J. I. Climente, M. Korkusinski, M. Scheibner, A. S. Bracker, P. Hawrylak, and D. Gammon, Phys. Rev. Lett. **102**, 047401 (2009).
[30] D. M. Ceperley and B. J. Alder, Phys. Rev. Lett. **45**, 566 (1980).
[31] J. P. Perdew and A. Zunger, Phys. Rev. B **23**, 5048 (1981).
[32] J. R. Chelikowsky, N. Troullier, and Y. Saad, Phys. Rev. Lett.

72, 1240 (1994).
[33] J. R. Chelikowsky, J. Phys. D **33**, R33 (2000).
[34] N. Troullier and J. L. Martins, Phys. Rev. B **43**, 1993 (1991).
[35] S. Cheong and M. Mostovoy, Nature Mater. **6**, 13 (2007).
[36] R. Ramesh and N. Spaldin, Nature Mater. **6**, 21 (2007).
[37] S. Ke, H. U. Baranger, and W. Yang, J. Chem. Phys. **126**, 201102 (2007).
[38] S. H. Ke, H. U. Baranger, and W. Yang, J. Chem. Phys. **127**, 144107 (2007).
[39] M. C. Beard, G. M. Turner, J. E. Murphy, O. I. Micic, M. C. Hanna, A. J. Nozik, and C. A. Schmuttenmaer, Nano Lett. **3**, 1695 (2003).
[40] P. Howard, A. Andreev, and D. A. Williams, Phys. Status Solidi C **5**, 3156 (2008).
[41] M. A. Reed, C. Zhou, C. J. Muller, T. P. Burgin, and J. M. Tour, Science **278**, 252 (1997).
[42] A. Salomon, D. Cahen, S. Lindsay, J. Tomfohr, V. B. Engelkes, and C. D. Frisbie, Adv. Mater. **15**, 1881 (2003).
[43] X. Li, J. He, J. Hihath, B. Xu, S. M. Lindsay, and N. Tao, J. Am. Chem. Soc. **128**, 2135 (2006).
[44] S. Lindsay, Faraday Discuss. **131**, 403 (2006).
[45] S. M. Lindsay and M. A. Ratner, Adv. Mater. **19**, 23 (2007).